

Reprinted from the Journal of the American Ceramic Society, Vol. 66, No. 7, July 1983  
Copyright 1983 by The American Ceramic Society

# Relation Between Multiregion Crack Growth and Dynamic Fatigue of Glass Using Indentation Flaws

P. CHANTIKUL<sup>\*,\*</sup>

Department of Applied Physics, School of Physics, University of New South Wales, New South Wales 2033, Australia

BRIAN R. LAWN,<sup>\*</sup> HERBERT RICHTER,<sup>†</sup> and STEPHEN W. FREIMAN<sup>\*</sup>

Fracture and Deformation Division, National Bureau of Standards, Washington, DC 20234

The influence of transport-limited kinetic crack growth on the fatigue properties of soda-lime glass was examined. Dynamic fatigue data were taken on specimens with controlled indentation flaws and were compared with the predicted response from measured crack velocity characteristics. Heptane was used as the operational test environment because of its pronounced crack velocity plateau; control tests in water served to establish a baseline reference for comparing the results. Fractographic observations using a stress wave marker technique showed a complex growth history for flaws broken in heptane compared to that for flaws broken in water. The magnitude of the predicted region II influence is too small to be detected in the dynamic fatigue results, even allowing for the relatively high degree of data reproducibility. The implications of this conclusion for lifetime predictions are discussed.

## I. Introduction

THE long-term strength of brittle solids is governed by such factors as flaw size and shape and the susceptibility to chemically enhanced slow crack growth. Implicit in the fracture mechanics treatments of time-dependent strength (fatigue) properties are certain assumptions concerning these factors, e.g. that the flaws respond in essentially the same way as macroscopic cracks and that the crack velocity can be expressed as some simple function (usually power law) of the stress intensity factor. The

success of this approach has led, in conjunction with statistical accountability of flaw populations, to useful engineering design schemes.<sup>1,2</sup>

This paper examines the degree to which macroscopic crack velocity data can be used to determine the kinetics of failure in strength testing. In particular, a critical look is taken at the potential complications in lifetime predictions when the crack velocity function shows multiregion behavior.<sup>3</sup> Generally, three such regions are identifiable: region I (low velocities), controlled by rate of reaction between environmental species and crack-tip bonds; region II (intermediate velocities), controlled by rate of transport of environmental species to the tip; region III (high velocities), controlled by electrostatic environment-bond interactions.<sup>4</sup> It is customary to recognize the existence only of region I in the formal derivation of fatigue equations, on the grounds that it is the domain of slowest growth that must control the crack evolution to failure and that in the more concentrated active environments (e.g. water) the higher regions are not strongly evident in the crack velocity response. In addition, it has been argued that natural surface flaws, by virtue of their relatively small size and their continuous accessibility to the external environment at the points of intersection with the free surface,<sup>5-7</sup> may not be subject to conventional region II effects. Considerations of this kind clearly raise questions about the status of macroscopically determined crack velocity functions as a suitable basis for fatigue strength analysis.

The approach adopted here is to run dynamic fatigue tests on glass specimens with controlled flaws, generated by Vickers indentations,<sup>6-11</sup> in an environment with a pronounced region II crack velocity plateau. Although indentation-induced crack systems are subject to intense residual stress fields,<sup>10,12,13</sup> these fields have been well characterized and are readily accommodated into the fracture mechanics formalism.<sup>6,14</sup> The element of control significantly reduces the statistical aspect, and allows for monitoring of the crack evolution to failure. In the present study, this monitoring is accomplished by imposing periodic stress markers onto the frac-

Received October 14, 1982; revised copy received February 11, 1983; approved February 21, 1983.

Supported by the U. S. Office of Naval Research, Metallurgy and Ceramics Program, and by the Deutsche Forschungsgemeinschaft.

<sup>\*</sup>Member, the American Ceramic Society.

<sup>\*</sup>Now with the Department of Physics, Chulalongkorn University, Bangkok, Thailand.

<sup>†</sup>On leave from Fraunhofer Institut für Werkstoffmechanik, Freiburg, Federal Republic of Germany.

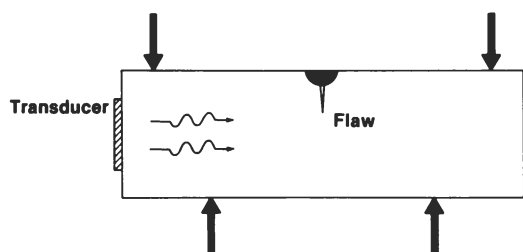


Fig. 1. Schematic of transducer setup for imposing sonic markers on surface of indentation flaw in flexural specimen.

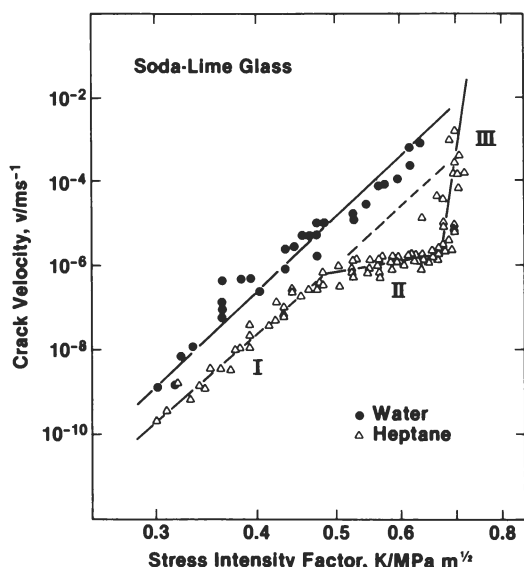


Fig. 2. Crack velocity data for soda-lime glass in heptane (6 specimens) and water (2 specimens) obtained using double-cantilever technique. For heptane, solid lines are segmented least-squares fits to regions I, II, and III; broken line is extrapolation of region I to point of intersection with region III. For water, solid line is prediction from fatigue data.

ture surfaces.<sup>15-17</sup> The dynamic fatigue data are then compared to predictions calculated from  $v$ - $K$  curves<sup>2</sup> obtained on double-cantilever-beam specimens.

## II. Experimental Procedure

Soda-lime glass was selected as a model material for all tests in this study. Heptane was chosen as the test medium because its low affinity for water ( $\approx 50$  ppm) leads to a wide region II plateau; also, it has been determined that exposure to air does not lead to an increase in water concentration. Control tests were conducted in water to provide a convenient reference baseline for data analysis. Inert strength tests for parameter calibration were conducted in dry nitrogen gas.<sup>6,7</sup>

### (1) Macroscopic Crack Velocity Measurements

Crack velocities were measured on specimens (75 by 12.5 by 1 mm) cut from glass microscope slides, using the double-cantilever configuration with applied-moment loading.<sup>18</sup> A groove  $\approx 0.5$  mm deep was cut down the length of one face to guide the crack. The specimens were annealed, precracked, and immersed in the test fluid. An optical microscope was used to monitor the crack growth. Stress intensity factors were calculated from the applied load and specimen dimensions.<sup>18</sup>

<sup>2</sup>The subscript is dropped from  $K_I$ , on the understanding that we are always dealing with mode I cracks.

### (2) Failure Tests on Controlled-Flaw Specimens

Controlled flaws for strength testing were introduced by indenting with a Vickers pyramid. Flaws of different dimensions were produced by varying the contact load,  $P$ , so that any size effect in the region II kinetics might be investigated.<sup>11</sup> All indentations were made in air at a fixed load duration of 10 s, and were left to stand for  $\approx 30$  min before strength testing to allow any relaxation in the residual stress field (e.g. due to lateral crack growth<sup>8</sup>) to equalize for all specimens.

The failure tests were conducted in four-point flexure, using a crosshead machine to deliver the bending loads. The rods were carefully oriented so that one set of radial cracks emanating from the indentation corners was normal to the maximum tensile stress. For water, a droplet was simply placed on the indentation site immediately prior to testing; in the case of heptane a liquid bath was necessary because of rapid evaporation. In the latter case the specimens were dried for several minutes in hot air before immersion. Beam theory was used to compute the stress at failure,  $\sigma_f$ . Routine microscopic examination of the broken parts was carried out to confirm that failure originated at the indentation flaw.

(A) *Stress Wave Fractography*: Stress wave fractographic observations<sup>15-17</sup> were made on annealed glass specimens (150 by 8 by 2 mm) containing 5 N indentations. A transducer mounted at the end of the bend bar generates transverse stress waves normal to the plane of the indentation crack which is to lead to failure (Fig. 1). These waves periodically modify the direction of the maximum tensile stress generated by the external load, without significantly affecting the driving force on the crack. The perturbations leave optically detectable time markers on the fracture surface. Taken in conjunction with the transducer frequency, the markers constitute a pictorial record of the velocity history of the crack system. The major departure from previous studies using this technique is in the lower frequencies attainable,  $< 0.1$  Hz (cf. the MHz region conventionally used); under such operating frequencies optically resolvable markers could be produced at crack velocities  $< 1 \mu\text{m/s}$ , corresponding to the heptane data plateau region.

(B) *Dynamic Fatigue Curves*: Fatigue tests were carried out at constant stressing rates,  $\dot{\sigma}_a$ , on annealed glass rods 5 mm in diam. (inner span 20 mm, outer span 60 mm). An effort was made to cover as wide a stressing-rate range as possible (e.g. by incorporating a piezoelectric load cell into the system for measuring flexural forces at fast rates)<sup>7</sup> to maximize the prospects of detecting any significant shifts in the comparative heptane and water fatigue curves. Inert strengths were measured at the fastest loading rates in flowing dry  $\text{N}_2$  gas.

## III. Results and Discussion

Let us now show the correspondence between the three sets of observations, i.e. macroscopic crack growth, fractography, and dynamic fatigue.

The macroscopic crack-growth data in Fig. 2 show clear evidence for multiregion velocity behavior in heptane. These data agree with those previously reported for heptane and other alkanes.<sup>19</sup> For a macroscopic crack, the level of the plateau is a function of the concentration of water and the viscosity of the fluid.<sup>4</sup> However, Quackenbush and Frechette<sup>20</sup> and Richter<sup>16</sup> showed that both the crack velocity at which a plateau is observed and the crack-front shape are functions of specimen thickness. The work of these authors suggests that the heptane  $v$ - $K$  curve in Fig. 2 is not unique. Whereas regions I and III represent reaction rates intrinsic to the material-environment system, region II is dependent on crack size and shape.

Now consider the flaw-growth patterns in Fig. 3 obtained by stress wave fractography on cracks grown under a constant bending load. In both Figs. 3(A) and 3(B), corresponding, respectively, to heptane and water, two frequencies have been superimposed to allow coverage of a wide range of velocities. First note that the markers for the specimen tested in water remain closely elliptical in profile, and increase smoothly in spacing, over the entire range of crack growth, corresponding to velocities from  $2 \mu\text{m/s}$  to

100 mm·s<sup>-1</sup>, indicative of a single region of crack propagation. The flaw growth in heptane is more complex. The spacing of the markers in the low-frequency domain is nearly constant, and corresponds to a crack velocity of 3 μm·s<sup>-1</sup>, near the region II plateau. As crack growth proceeds within this region, the crack front becomes increasingly distorted from its initially near-elliptical profile below the tensile surface. Once into the high-frequency domain, corresponding to velocities >1 m·s<sup>-1</sup>, the front reverts to the elliptical geometry. This difference in behavior between water and heptane environments was reproducible over a number of tests.

Based on the preceding fractographic observations, it would be expected that the fatigue strengths of specimens tested under water and heptane might differ, especially at stressing rates for which the crack spends the largest portion of its growth in region II.

Accordingly, let us examine the possible correspondence between  $v$ - $K$  and dynamic fatigue results in terms of indentation fracture mechanics. All mathematical details involved in establishing this correspondence are relegated to the Appendix. We simply note at this point that analytical solutions of the fatigue equations for flaws with residual stresses are obtainable only for single-region crack velocity functions of power-law form, and that these solutions are themselves of power-law form.<sup>14</sup> Figure 4 shows the dynamic fatigue curves predicted from the crack-growth data in heptane, with and without a region II plateau included in the calculations, as well as the experimental dynamic fatigue data in water and heptane. Note that the data have been normalized for indentation load,  $P$ , so that all data for each environmental condition might be reduced to a universal curve.

The sequence of operations to obtain the predicted and measured dynamic fatigue curves in Fig. 4 was as follows:

(i) On the assumption that the results for tests in water may be described by single-region behavior over the data range covered, a linear least-squares fit was appropriately made to the logarithmically plotted dynamic fatigue data<sup>11</sup> in Fig. 4. The slope and intercept of this fitted line, in conjunction with inert strength parameters, gives, via a suitable set of transformation equations, corresponding values for exponent and coefficient in the glass/water crack velocity equation.

(ii) A linear representation of the result from step (i) was made on the logarithmic crack-velocity/stress-intensity-factor diagram, Fig. 2. The plotted line is seen to pass through the experimental points for a water environment, within the scatter over the data range covered.<sup>8</sup> Thus self-consistency between results from fatigue and velocity tests is established for this single-region system.

(iii) Linear least-squares fits were made to each of the three clearly defined crack velocity regions in Fig. 2. Appropriate exponents and coefficients were evaluated for each fitted segment.

(iv) Using these calibrated velocity parameters, together with the same inert-strength parameters referred to in (i), numerical solutions<sup>12</sup> were obtained for the dynamic fatigue equation (Appendix) for heptane.<sup>1</sup> Two such solutions are plotted in Fig. 4, one with and the other without region II included in the crack velocity function; in the latter case region I is taken to operate up to the extrapolated intersection with the region III curve (Fig. 2).

Even with the relatively high degree of reproducibility achieved by using indentation-induced flaws, the magnitude of any region II influence seems to be too small to be unequivocally distinguished in the dynamic fatigue results for heptane. The fact that the data taken at different loads fall onto the same curve for each environment indicates that flaw size alone is not a primary factor. Similar conclusions were reported by Chandan *et al.*,<sup>5</sup> although their data were less detailed than those presented here.

#### IV. Concluding Remarks

The foregoing observations suggest that indentation flaws do not show a one-to-one correspondence with macroscopic cracks in their multiregion crack velocity response. This breakdown in correspondence appears to be confined to region II; we recall that for the tests in water, where region I effectively controls the kinetics over the data range considered, mutual consistency is obtained between crack velocity and dynamic fatigue results. Regions I and

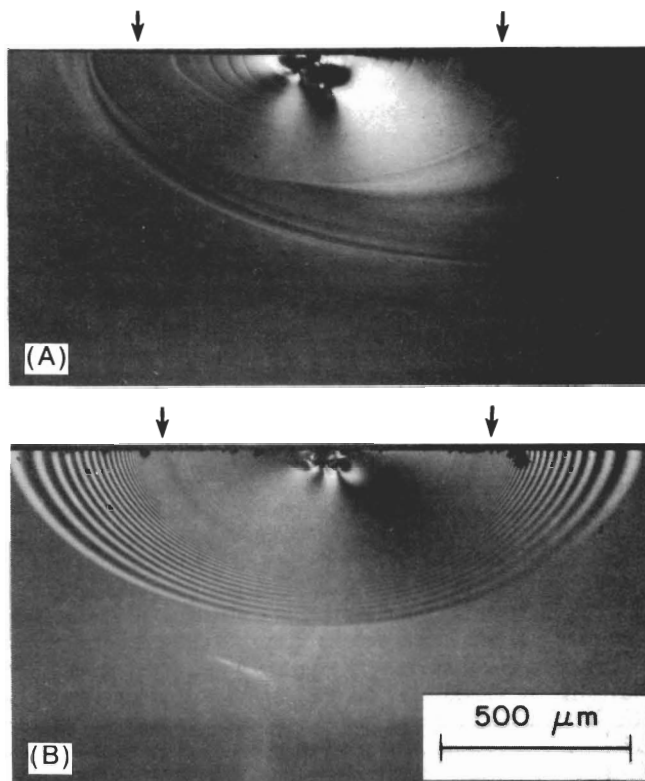


Fig. 3. Fracture surfaces of soda-lime glass from indentations at contact load of 5 N and subsequent bending stress of 35 MPa: (A) heptane, marker frequencies 60 MHz and 104 kHz; (B) water, 1.1 Hz and 1.9 kHz. (Superposed frequencies in each case simply allow coverage of extended velocity range; arrows indicate points at which markers correspond to transition from lower to higher frequency.) Compare distorted marker pattern in heptane with relatively symmetrical pattern in water.

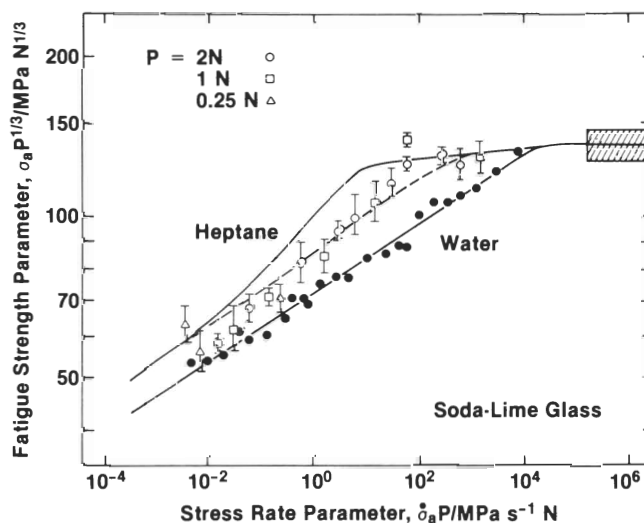


Fig. 4. Normalized dynamic fatigue curves for soda-lime glass in heptane and water. Each data point is mean and standard deviation, in logarithmic coordinates, of 6 to 15 specimens (error bars omitted for water, for clarity). Contact loads  $P$  used for heptane are indicated (loads used to obtain control water data covers range 0.05 to 10 N (Ref. 11), but are not differentiated here). Shaded band denotes inert-strength level. Solid line through water data is least-squares fit. Solid line through heptane data is prediction from crack velocity curve with region II included; broken line is corresponding prediction with region II excluded.

<sup>8</sup>In drawing a straight line through the water data in Fig. 2 we intend no statement about the fundamental relation between crack velocity and stress intensity factor; ours is strictly an empirical fitting procedure.

<sup>14</sup>Inclusion of a possible threshold stress intensity factor at 0.3 MPa·m<sup>1/2</sup> in Fig. 2 did not significantly affect the calculated fatigue curves.

III are intrinsic to the material/environment and would not be expected to depend in any way on crack geometry. For region II, however, with its origins deeply rooted in transport mechanisms, geometrical factors must play some role. Such effects have been noted in fracture mechanics specimens, where the crack velocity plateau becomes a function of specimen width.<sup>16,20</sup> Our results suggest that crack *shape* is an even more important factor than crack *size*. Thus, in the present instance with axisymmetric contact loading the crack system always has a surface trace in direct contact with the environment, so transport effects are apparent only in the subsurface propagation; region II effects are then manifested as a constraint on the surface expansion by the more slowly moving inner crack portions.

The heptane results in Fig. 2 seem to indicate that higher regions in the crack velocity function are unlikely to influence fatigue properties strongly, particularly in longer-term tests, where the crack spends nearly all its growth time in region I. This is not altogether unexpected, bearing in mind the smoothing effect of integrating over the crack velocity function in the failure mechanics. Nevertheless, care should be taken in extrapolating fatigue data to long lifetime domains which lie well outside the data range. Fortunately, the conventional linear extrapolation procedure (i.e. without due regard to the curvature in the fatigue plot caused by higher regions) will tend to underestimate lifetimes, in line with the requirements of conservative design.

Finally, we should point out that the insensitivity to region II effects discussed here may not extend to all strength-test procedures. In proof testing, the position and slope of region II have been shown to significantly affect subsequent strength distributions. The difference between proof testing and dynamic fatigue is that, in the latter, the failure stress is controlled more by the lower end of the crack velocity spectrum through which the flaw grows, whereas in the former it is only the higher end which controls. A detailed description of proof testing in this context will be given elsewhere.<sup>21</sup>

## APPENDIX

In this Appendix a summary is given of the derivation of dynamic fatigue equations from the crack velocity function for flaws with residual contact stress. Reference is made to earlier papers for more detailed formulations.<sup>6,11,14</sup>

The analysis begins with the assumption that the crack velocity  $v$  relates to the stress intensity factor  $K$  via a power law,

$$v = v_0(K/K_c)^n \quad (\text{A-1})$$

where  $n$  and  $v_0$  are empirical exponent and coefficient, respectively, for a given material/environment system and  $K_c$  is the material toughness. For cracks of characteristic dimension  $c$  produced at a peak indentation load  $P$  and subjected to subsequent tensile stress  $\sigma_a$ , the stress intensity factor has the form

$$K = \chi P/c^{3/2} + \psi \sigma_a c^{1/2} \quad (\text{A-2})$$

where  $\chi$  and  $\psi$  are dimensionless constants; the first term in Eq. (A-2) represents the residual contact field and the second represents the applied field. In dynamic fatigue testing the stressing rate is held constant as a function of time  $t$ , i.e.

$$\sigma_a = \dot{\sigma}_a t \quad (\dot{\sigma}_a = \text{constant}) \quad (\text{A-3})$$

Combining the above three equations gives

$$dc/dt = v_0(\chi P/K_c c^{3/2} + \psi \dot{\sigma}_a c^{1/2}/K_c)^n \quad (\text{A-4})$$

which serves as a master differential equation. Solution of this equation involves computation of the time-to-failure,  $t_f$ , i.e. the time for the crack to grow from its original size to a critical instability configuration ( $K = K_c$ ,  $dK/dc > 0$ ), thereby defining the failure strength,  $\sigma_f = \dot{\sigma}_a t_f$ .

Solutions of *analytical* form are obtainable from Eq. (A-4) only for single-region crack velocity functions. For the case where  $P$  is used as a test variable, these solutions are of power-law form<sup>11,14</sup>

$$\sigma_f P^{1/3} = (\lambda_P' \dot{\sigma}_a P)^{1/(n'+1)} \quad (\text{A-5})$$

with exponent and coefficient which relate to the crack velocity parameters in Eq. (A-1) via the "transformation equations"<sup>14</sup>

$$n = 4n'/3 - 2/3 \quad (\text{A-6a})$$

$$v_0 = (2\pi n')^{1/2} (\sigma_m P^{1/3})^{n'} (c_m/P^{2/3})/\lambda_P' \quad (\text{A-6b})$$

The quantities labeled with subscript  $m$  in Eq. (A-6b) refer to the conditions under *equilibrium* crack growth, i.e. with  $K = K_c$ ,  $dK/dc = 0$  in Eq. (A-2), whence

$$\sigma_m P^{1/3} = 3K_c^{4/3}/4^{4/3}\psi(\chi P)^{1/3} \quad (\text{A-7a})$$

$$c_m/P^{2/3} = (4\chi P/K_c)^{2/3} \quad (\text{A-7b})$$

These instability conditions are measurable as the strength and corresponding crack size in inert environments.<sup>6,7</sup> Thus from Eq. (A-5) we see that a plot of  $\log(\sigma_f P^{1/3})$  vs  $\log(\dot{\sigma}_a P)$  should be universally linear for all contact loads.

For multiregion crack velocity functions no such analytical solutions are available. It is then necessary to integrate Eq. (A-4) *numerically* over the crack velocity range.<sup>6</sup>

**Acknowledgments:** The authors thank E. R. Fuller and S. M. Wiederhorn for discussions and T. P. Dabbs and A. C. Gonzalez for collecting some of the data.

## References

- <sup>1</sup>S. M. Wiederhorn, pp. 613–46 in *Fracture Mechanics of Ceramics*, Vol. 2. Edited by R. C. Bradt, D. P. H. Hasselman, and F. F. Lange. Plenum, New York, 1974.
- <sup>2</sup>S. M. Wiederhorn and J. E. Ritter, pp. 202–14 in *Fracture Mechanics Applied to Brittle Materials*. Edited by S. W. Freiman. *ASTM Spec. Tech. Publ.*, No. 678, 1979.
- <sup>3</sup>S. M. Wiederhorn, "Influence of Water Vapor on Crack Propagation in Soda-Lime Glass," *J. Am. Ceram. Soc.*, **50** [8] 407–14 (1967).
- <sup>4</sup>S. M. Wiederhorn, S. W. Freiman, E. R. Fuller, Jr., and C. J. Simmons, "Effects of Water and Other Dielectrics on Crack Growth," *J. Mater. Sci.*, **17** [12] 3460–78 (1982).
- <sup>5</sup>H. C. Chandan, R. C. Bradt, and G. E. Rindone, "Dynamic Fatigue of Float Glass," *J. Am. Ceram. Soc.*, **61** [5–6] 207–10 (1978).
- <sup>6</sup>B. R. Lawn, D. B. Marshall, G. R. Anstis, and T. P. Dabbs, "Fatigue Analysis of Brittle Materials Using Indentation Flaws: I," *J. Mater. Sci.*, **16** [10] 2846–54 (1981).
- <sup>7</sup>R. F. Cook, B. R. Lawn, and G. R. Anstis, "Fatigue Analysis of Brittle Materials Using Indentation Flaws: II," *J. Mater. Sci.*, **17** [4] 1108–16 (1982).
- <sup>8</sup>D. B. Marshall and B. R. Lawn, "Flaw Characteristics in Dynamic Fatigue: The Influence of Residual Contact Stresses," *J. Am. Ceram. Soc.*, **63** [9–10] 532–36 (1980).
- <sup>9</sup>P. Chantikul, B. R. Lawn, and D. B. Marshall, "Micromechanics of Flaw Growth in Static Fatigue: Influence of Residual Contact Stresses," *J. Am. Ceram. Soc.*, **64** [6] 322–25 (1981).
- <sup>10</sup>B. R. Lawn, A. G. Evans, and D. B. Marshall, "Elastic/Plastic Indentation Damage in Ceramics: The Median/Radial Crack System," *J. Am. Ceram. Soc.*, **63** [9–10] 574–81 (1980).
- <sup>11</sup>T. P. Dabbs, B. R. Lawn, and P. L. Kelly, "A Dynamic Fatigue Study of Soda-Lime Silicate and Borosilicate Glasses Using Small Scale Indentation Flaws," *Phys. Chem. Glasses*, **23** [2] 58–66 (1982).
- <sup>12</sup>D. B. Marshall and B. R. Lawn, "Residual Stress Effects in Sharp Contact Cracking: I," *J. Mater. Sci.*, **14** [8] 2001–12 (1979).
- <sup>13</sup>D. B. Marshall, B. R. Lawn, and P. Chantikul, "Residual Stress Effects in Sharp Contact Cracking: II," *J. Mater. Sci.*, **14** [9] 2225–35 (1979).
- <sup>14</sup>E. R. Fuller, B. R. Lawn, and R. F. Cook, "Theory of Fatigue for Brittle Flaws Originating from Residual Stress Concentrations," *J. Am. Ceram. Soc.*, **66** [5] 314–21 (1983).
- <sup>15</sup>F. Kerkhof, pp. 303–21 in *Linear Fracture Mechanics*. Edited by G. C. Sih, R. P. Wei, and F. Erdogan. Envo Publishing Co., Lehigh Valley, PA, 1974.
- <sup>16</sup>H. Richter, pp. 447–57 in *Proceedings of Eleventh International Congress on Glass*, Vol. 2. Edited by J. Gotz, C. V. T. S., Prague, 1977.
- <sup>17</sup>T. A. Michalske, V. D. Frechette, and R. Hudson, pp. 1091–97 in *Advances in Fracture Research*, Vol. 2. Edited by D. Francis. Pergamon, New York, 1981.
- <sup>18</sup>S. W. Freiman, D. R. Mulville, and P. W. Mast, "Crack Propagation Studies in Brittle Materials," *J. Mater. Sci.*, **8** [11] 1527–33 (1973).
- <sup>19</sup>S. W. Freiman, "Effect of Straight-Chain Alkanes on Crack Propagation in Glass," *J. Am. Ceram. Soc.*, **58** [7–8] 339–40 (1975).
- <sup>20</sup>C. L. Quackenbush and V. D. Frechette, "Crack-Front Curvature and Glass Slow Fracture," *J. Am. Ceram. Soc.*, **61** [9–10] 402–406 (1978).
- <sup>21</sup>S. M. Wiederhorn, S. W. Freiman, E. R. Fuller, Jr., and H. Richter, "Effect of Multiregion Crack Growth on Proof Testing," unpublished work.